Modelling residual stresses in weldments of work-hardened aluminum alloys with microstructural effects

E. Sarrazin, Ky Dang Van, Habibou Maitournam

Modelling residual stresses in weldments of work-hardened aluminum alloys with microstructural effects

E. Sarrazin, K. Dang Van and H. Maitournam

Laboratoire de Mécanique des Solides
Ecole Polytechnique
91128 Palaiseau Cedex, France

ABSTRACT

A model describing thermal, metallurgical and mechanical effects of welding is developed for work-hardened aluminium alloys. It is based on thermo-mechanical constitutive equations of a generalised standard elastoplastic type which, in addition, account for a metallurgical parameter. This parameter is used to describe recrystallisation kinetics of cold-rolled aluminium alloys and its effects on mechanical properties during welding. The constitutive relations are used in a finite-element code with a view to modelling metal inert gas (MIG) welds of 5086-H24 aluminium alloy plates. At each stage of the calculation, experimental verifications have been made to validate the numerical results : temperature, metallurgical transformations and residual stress fields. A good agreement between experimental and theoretical results (thermal cycle, width of heat affected zone (HAZ) and residual stresses) is obtained. The X-ray diffraction and incremental hole-drilling methods have been also used to measure residual stresses.

INTRODUCTION

Aluminium alloys are widely used as structural materials in welded assemblies. Welding operations create microstructural changes and residual stresses which need to be quantified for estimating margins in static or dynamic dimensioning. Thermo-mechanical simulations of the welding process taking into account microstructural effects have not so far been treated in aluminium alloys and constitute the objective of this paper.

During welding, aluminium alloys undergo severe softening in the heat affected zone (HAZ) due to recrystallisation of work-hardened aluminium alloys (5xxx series) or to dissolution and growth of precipitates in age-hardened alloys (2xxx and 6xxx series). Martukanitz[1], Shercliff and Ashby[2,3] and Myhr and Grong[4,5] have evaluated final microstructural distributions in age-hardened alloys such as 6xxx series. That kind of study has not been performed in 5xxx alloys. Moreover, calculation of residual stresses has not been carried out with aluminium alloys.

There is thus a need for an accurate simulation of the welding process in these aluminium alloys. During welding, temperature distribution, micro-structure and stress change in a complex manner due to coupled effects. According to the schematic figure first proposed by Inoue and Wang[6] for steels these three quantities are coupled as shown on Fig. 1. The temperature is affected by latent heat originating from recrystallisation or dissolution and by heat generation due to deformation which is small. The microstructure depends on temperature variations and deformation-induced transformation. Stress field varies by modification of mechanical properties with temperature and microstructure. Hence thermal–metallurgical–mechanical constitutive relations have to be established to model welding in aluminium alloys.

The purpose of this paper is to establish these constitutive relations for work-hardened alloys of the 5xxx type. They are based on thermo-mechanical constitutive equations of generalised standard elastoplastic type accounting for

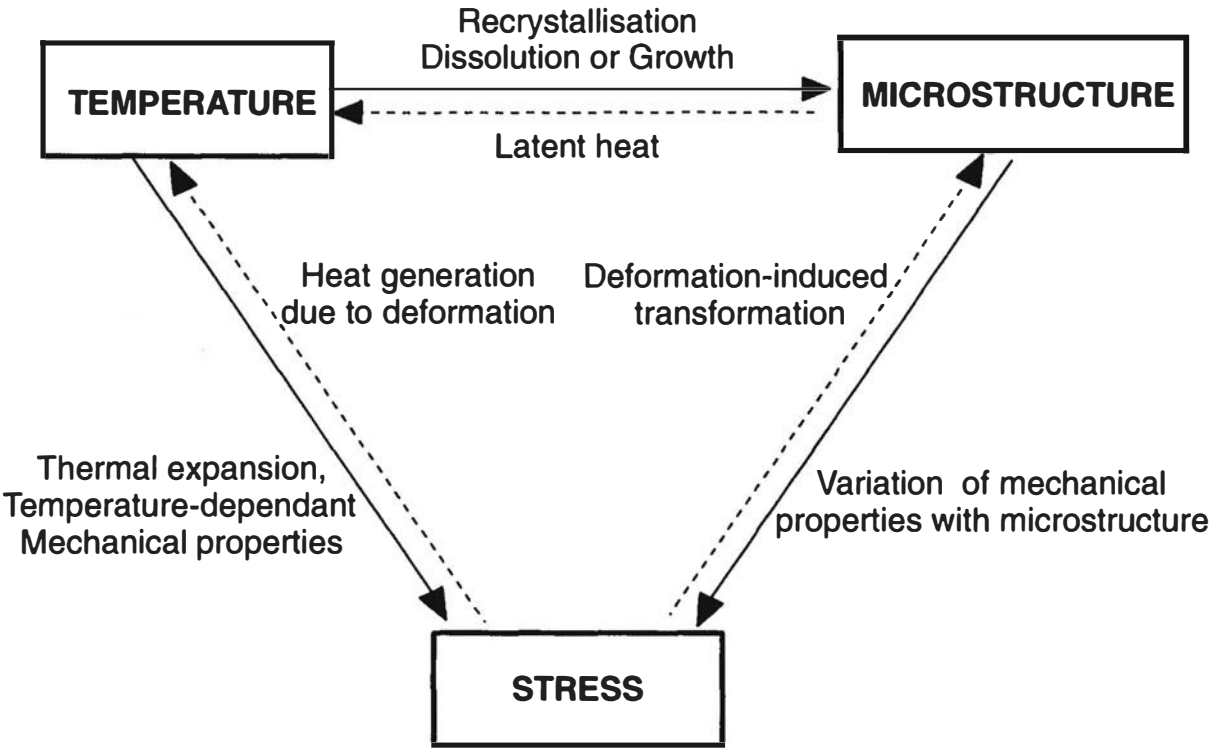

Figure 1. Coupling between temperature, metallic and stress structures during welding.

a metallurgical parameter which represents recrystallisation. Interactions sketched with dashed lines (latent heat, stress-induced transformation and heat dissipation) will be neglected. First, an analysis is carried out on the reaction governing recrystallisation in the HAZ during welding to derive recrystallisation kinetics. Then the contribution of recrystallisation on mechanical properties of the alloy is described to obtain constitutive equations with structural change. The resulting kinetics and constitutive laws are calibrated by isothermal experiments and mechanical tests, respectively. Finally, the model is numerically applied to predict recrystallisation in the HAZ and residual stresses in weld MIG of a cold-rolled 5086 (Al-4Mg-0.4Mn) alloy.

MODEL DESCRIPTION

Constitutive equations combining thermal, metallurgical and mechanical phenomena may be developed through the use of relationships describing the rate of recrystallisation associated with the temperature elevation and relations between recrystallisation and mechanical properties.

TRANSFORMATION KINETICS DUE TO RECRYSTALLISATION

When a cold-rolled material is welded, the effects of work-hardening are completely lost in the fusion zone due to melting and solidification and are partially lost in the HAZ due to recovery, recrystallisation and grain growth. During recrystallisation, the deformed grains are transformed into fresh and strain-free grains. Before recrystallisation takes place, however, if metal is heated to a temperature below that required for recrystallisation, the occurring process is recovery. During this process, dislocations move to form irregular cells. This could happen away from the fusion line. On the other hand, if temperature is higher, recrystallisation can be followed by grain growth close to the fusion zone. The microstructure of a work-hardened aluminium alloy may be illustrated by the schematic Fig. 2. Since the mechanical properties of the material, such as strength or hardness, do not change significantly during recovery and grain growth (Fig. 3), only recrystallisation will be taken into account. Recrystallisation is controlled by nucleation and growth transformations.[8] New grains nucleate and grow until the whole metal consists of undeformed grains. Let N be the rate of nuclei formation and G the growth rate of nuclei. The radius of precipitates is $r = Gt$, thus the volume of a sphere nucleated at $t = 0$ is

$$V = \frac{4}{3}\pi(Gt)^3 \tag{1}$$

If the particle does not nucleate until time (t-τ), and is observed at some later time t, the volume is

$$V_\tau = \frac{4}{3}\pi G^3(t-\tau)^3 \tag{2}$$

If the nucleation rate is constant, the number $Nd\tau$ of nuclei are formed in a unit volume. Thus if the particles do not impinge on one another, the volume fraction of recrystallised material is

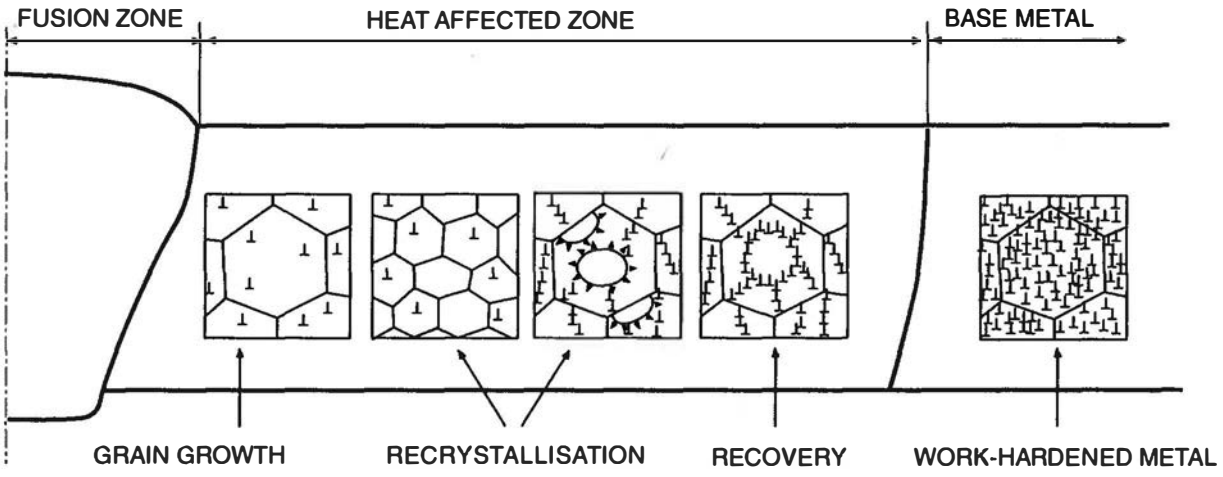

Figure 2. Microstructure in work-hardened aluminium alloys.

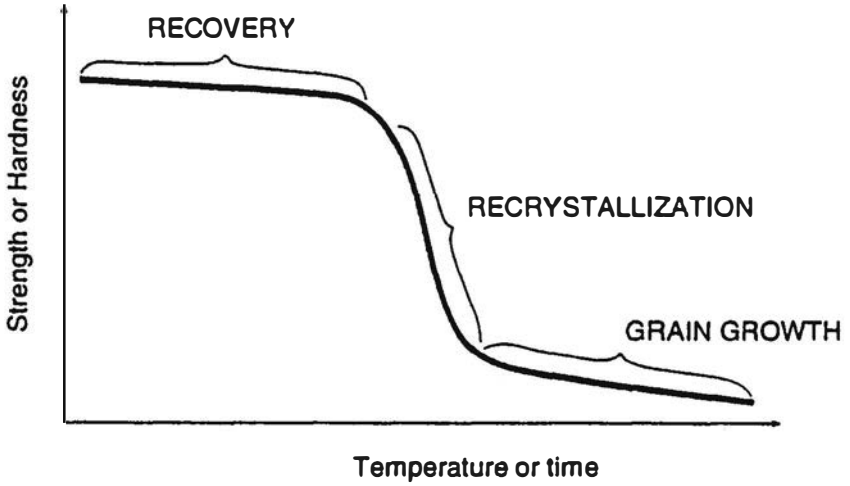

Figure 3. Schematic effect of recovery, recrystallization and grain growth on strength or hardness.[7]

$$m = \sum V_\tau = \frac{4}{3}\pi N G^3 \int_0^t (t-\tau)^3 \, d\tau = \frac{1}{3}\pi N G^3 t^4 \quad \text{for} \quad m \ll 1 \tag{3}$$

Equation (3) is valid only for short times, that is, before the particles interfere with one another's growth. The equation applicable to randomly distributed nuclei and valid for all times is

$$m = 1 - \exp\left(-\frac{\pi N G^3 t^4}{3}\right) \tag{4}$$

Nucleation rate N and growth rate G depend on temperature according to

$$N = N_0 \exp\left(-\frac{Q_N}{RT}\right) \tag{5}$$

$$G = G_o \exp\left(-\frac{Q_G}{RT}\right) \tag{6}$$

where N_0 and G_o are constants, while Q_N and Q_G are the activation energy for nucleation and growth respectively. Thus equation (4) can be written as

$$m = 1 - \exp\left[-\frac{\pi N_o G_o^3 t^4}{3} \exp\left(-\frac{Q_N + 3Q_G}{RT}\right)\right] \tag{7}$$

Rearranging this equation, we choose to identify isothermal kinetics of recrystallization defined by

$$m = 1 - \exp\left(-\left[l\, t \exp\left(-\frac{Q_r}{RT}\right)\right]^\beta\right) \tag{8}$$

where the values of the global activation energy of recrystallisation Q_r and the parameters β, l are determined through isothermal experiments in salt baths. These experiments have been conducted to simulate welding conditions as closely as possible. They involve heating samples to various temperatures between 280 and 500°C maintained for short durations from 10 to 1800 s.

To apply the isothermal reaction kinetics[8] to continuous welding thermal cycle, it has been found that the transformation should follow an additivity rule. Under these conditions, it is assumed that the reaction would take the same course, except for the time scale, regardless of the temperature path. Avrami[9,10] has shown that the reaction is additive when it is isokinetic, i.e. when the nucleation rate is proportional to the growth rate. However, Cahn[11] found that systems in which nucleation occurs early in the reaction also verify the additivity rule. Equation (7) shows that the transformed fraction depends primarily on the growth rate G and secondarily on nucleation rate N. Thus, we assume that the recrystallisation reaction obeys the additivity rule. Under these

conditions, the reaction rate is solely a function of the transformed fraction m and temperature T, that is

$$\dot{m} = g(m, T) \tag{9}$$

Using Equation (8), it follows that the reaction during a continuous thermal cycle has the following form

$$\dot{m} = \beta l \exp\left(-\frac{Q_r}{RT}\right)[-\ln(1-m)]^{1-1/\beta}(1-m) \tag{10}$$

CONTRIBUTION OF RECRYSTALLISATION ON MECHANICAL PROPERTIES

It is generally assumed that the volume fraction of recrystallised metal is related to its hardness H by

$$m = \frac{H - H_i}{H_f - H_i} \tag{11}$$

where H_i is the initial hardness of unrecrystallised metal and H_f is the final hardness of completely recrystallised metal. But Equation (11) is not sufficient to characterise yield strength and hardening modulus. Hence, we performed mechanical testing on the 5086-H24 alloy used for welding, with a view to determining constitutive relations valid in the ranges of temperatures, strains and microstructural states associated with welding. Uniaxial tension-compression tests have been performed on plate specimens for temperatures from 20 to 500°C and for strains from 0 to 0.02. These tests are performed at a strain rate of $\dot{\epsilon} = 10^{-3}s^{-1}$, and for five microstructural states (0, 20, 50, 90, and 100 % recrystallisation respectively). Heating and mechanical loading are short enough duration to assume constant microstructure during the test.

The strain–stress diagrams obtained[12] show that the thermo-mechanical behaviour of the metal can be modelled by elastoplastic constitutive equations with kinematic linear hardening. Apart from this experiment, we established that yield strength and hardening modulus of the metal are proportional to the square of the recrystallised fraction.

To account for the coupling effects during welding, it is necessary to use continuum thermodynamics. Total strain rate $\dot{\epsilon}$ is divided into the elastic strain rate $\dot{\epsilon}^e$ and the plastic strain rate $\dot{\epsilon}^p$ within the framework of the infinitesimal theory, that is

$$\dot{\epsilon} = \dot{\epsilon}^e + \dot{\epsilon}^p \tag{12}$$

The thermodynamic state of the alloy during welding is assumed to be characterised by temperature T, thermal elastic strain rate $\dot{\epsilon}^e$, plastic strain rate $\dot{\epsilon}^p$ and volume fraction due to recrystallisation m.

Following the usual procedure of the internal variable theory of thermodynamics, we get the constitutive relations from the free energy $\psi = \psi(\dot{\epsilon}^e, \dot{\epsilon}^p, T, m)$ and dissipation inequality. The entropy s, the stress σ, kinematic hardening X and the microstructural parameter M associated with m, have the form

$$s = -\frac{\partial \Psi}{\partial T} \qquad \sigma = \rho \frac{\partial \Psi}{\partial \epsilon^e} \qquad \mathbf{X} = \rho \frac{\partial \Psi}{\partial \epsilon^p} \qquad M = \rho \frac{\partial \Psi}{\partial m} \tag{13}$$

The elastic strain rate is given by Hooke's law

$$\dot{\epsilon}^e = \frac{1+\nu}{E}\dot{\sigma} - \frac{\nu}{E}\,\mathrm{tr}\,(\dot{\sigma})\mathbf{I} + \alpha T \mathbf{I} \tag{14}$$

where E is the Young modulus, ν the Poisson coefficient and α the expansion coefficient. The plastic strain rate is determined by the flow rule

$$\dot{\epsilon}^p = \Lambda \frac{\partial F}{\partial \sigma} \tag{15}$$

where F is the yield function reduced to the kinematic case and to the deviatoric stress $S = \sigma - \frac{1}{3} tr(\sigma)\mathbf{I}$

$$F = \sqrt{\frac{3}{2}(\mathbf{S}-\mathbf{X}) : (\mathbf{S}-\mathbf{X})} - k(T,m) \quad \text{where } k(T,m) = k_i + (k_f - k_i)\sqrt{m} \tag{16}$$

Assuming linear kinematic hardening, the evaluation of the centre X of the yield surface is governed by

$$\mathbf{X} = \frac{2}{3} C(T,m)\dot{\epsilon}^p \quad \text{where} \quad C(T,m) = C_i + (C_f - C_i)\sqrt{m} \tag{17}$$

Also, the plastic multiplier Λ satisfies the following relations

$$\Lambda \geq 0 \quad \text{and} \quad F\Lambda = 0 \tag{18}$$

It is determined by the consistency relation

$$\dot{F} = 0 \quad \text{and} \quad F = 0 \tag{19}$$

Summarising and combining the previous equations, the constitutive law takes the form*

* $H(f)$ is the Heaviside function: $H(F) = 0$ if $F < 0$, $H(F) = 1$ if $F = 0$
$< \ . \ >$ designs positive part: $< u >= 0$ if $u < 0$ and $< u >= u$ if $u \geq 0$.

$$\dot{\epsilon} = \dot{\epsilon}^e + \dot{\epsilon}^p \tag{20}$$

$$\dot{\epsilon}^e = \frac{1+\nu}{E}\dot{\sigma} - \frac{\nu}{E}\,\mathrm{tr}\,(\dot{\sigma})\mathbf{I} + \alpha \dot{T}\mathbf{I} \tag{21}$$

$$\dot{\epsilon}^p = \frac{9H(F)}{4}\frac{<(\mathbf{S}-\mathbf{X}):\dot{\sigma}>(\mathbf{S}-\mathbf{X})}{[C_i+(C_f-C_i)\sqrt{m}]\,[k_i+(k_f-k_i)\sqrt{m}]^2} \tag{22}$$

$$\mathbf{X} = \frac{2}{3}[C_i+(C_f-C_i)\sqrt{m}]\dot{\epsilon}^p \tag{23}$$

Parameters E, k_i, k_f, C_i, C_f are calibrated in function of temperature by means of mechanical tests. ν and α are assumed constant and equal to 0.3 and $25.10^{-6}\,K^{-1}$ respectively.

APPLICATION OF THE MODEL TO THE WELDING PROCESS

Analysis of temperatures, recrystallisation, and stresses are carried out based on the theory and the data discussed in the previous sections. The application is MIG-welding of two plates ($6\times150\times400\,mm^3$) of a 5086-H24 alloy (Fig. 4). The weld is performed in one pass with a 5356 filler alloy in a V groove preparation. Fixtures are used to maintain the weldments horizontally without preventing them from moving in the plane (OXY).

A numerical analysis of thermal, metallurgical and mechanical response due to welding is performed by use of the finite element method. Due to symmetry, only one half of the plate is modelled. Two-dimensional numerical simulations have been carried out:

- in a transverse cross-section perpendicular to the welding direction, under generalised plane strain assumption ($\epsilon_{yy} \neq 0$) ;

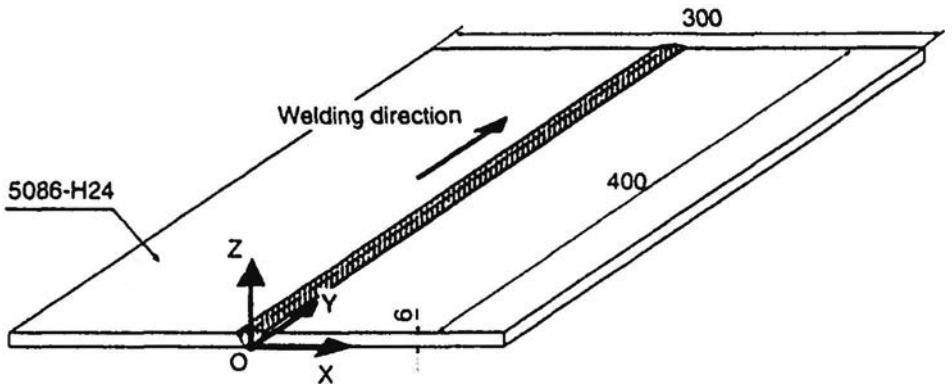

Figure 4. Geometry of the Weldments.

- in the longitudinal X–Yplane parallel to the welding direction, under plane stress assumption ($\sigma_{zz} = 0$).

The numerical calculations of the welding process is divided into three parts : thermal, microstructural and mechanical analysis. First temperatures are computed and compared to measurements by thermocouples. Then the distribution of temperature is used to compute microstructural changes due to recrystallisation in the HAZ. The predicted amount of recrystallised fraction is compared to experimental measurements on cross-sections. Finally, based on temperature and structural distributions thus obtained, stresses are analysed and compared to experimental values determined by the X-ray diffraction method and the hole-drilling technique.

THERMAL CALCULATION

The temperature distribution in the weldments is governed by the heat equation. Regarding assumptions on the fact that dissipative phenomenon and latent heat due to recrystallisation have little influence to welding, the heat equation states that the rate of change of heat due to storage $\rho C_p T$ and conduction $\mathrm{div}(-\lambda \mathrm{grad} T)$ may be in equilibrium with the heat production r

$$\rho C_p T - \mathrm{div}(\lambda \ \mathrm{grad} \ T) = r \tag{24}$$

The thermal capacity C_p is temperature dependent and includes latent heat originating from liquid–solid phase changes in the temperature interval bounded by the solidus and liquidus temperatures. The thermal conductivity λ also depends on temperature; it is artificially raised in the molten metal with a view to accounting for convection and homogenised temperature in the weld pool. The heat input r is modelled by a volumic heat flow introduced in the fusion zone. The experimental value for the weld power

$$Q = \eta UI \tag{25}$$

is known, where I is the normal current, U is the arc voltage and η is an arc efficiency. For the transverse model (OXY plane), this heat is introduced in the weld pool as a Gaussian repartition during a time τ which is determined by the ratio of the the weld pool length to the welding speed. The coefficient η has to be adjusted to obtain the good localisation of the fusion contour of the melted zone. For the longitudinal model (OXZ plane), the effect of velocity of the torch is taken into account under steady state conditions, thus we just have to evaluate the efficiency η. The cooling boundary conditions result from convection and radiation in the air and by conduction through fixtures.

Contours and temperature history at four distances from the weld line are plotted in Figs. 5 and 6. The calculated curves agree very well with the experimental data measured by thermocouples.

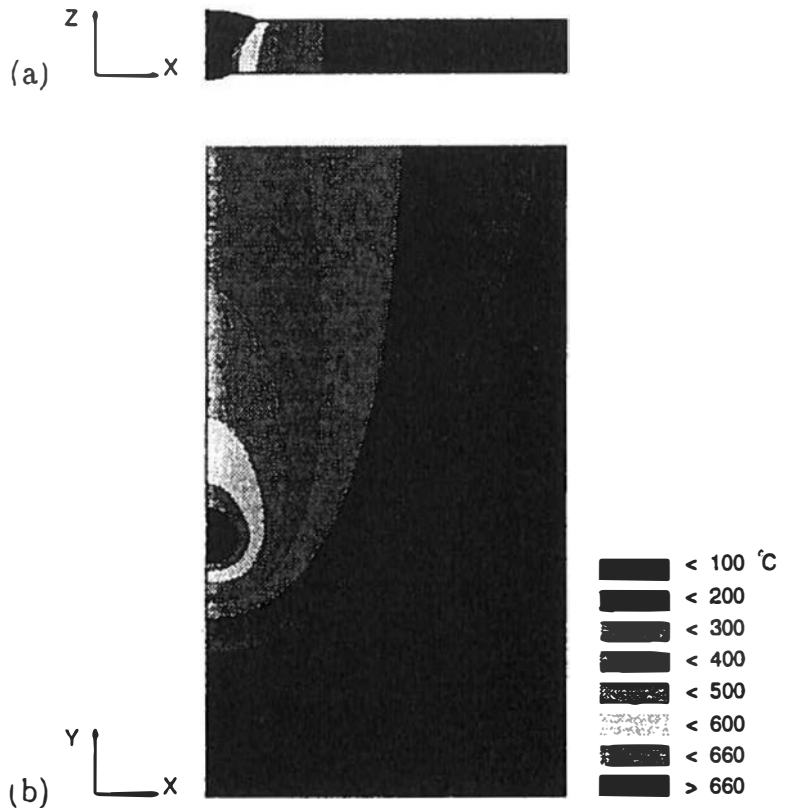

Figure 5. Contours of temperature for the transverse model (a) and the longitudinal model (b).

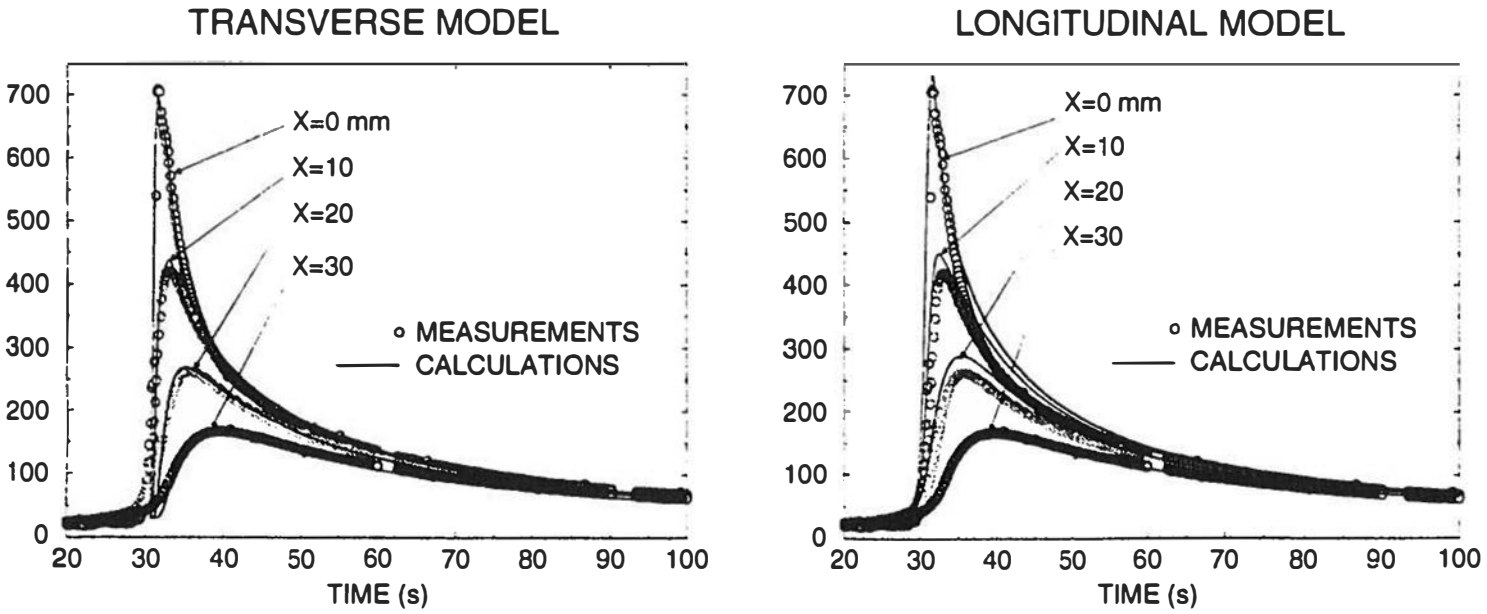

Figure 6. Temperature distribution.

MICROSTRUCTURAL CALCULATION

Calculation of the evolution of the volume fraction due to recrystallisation is based on anisothermal kinetics detailed in Equation (10) The numerical

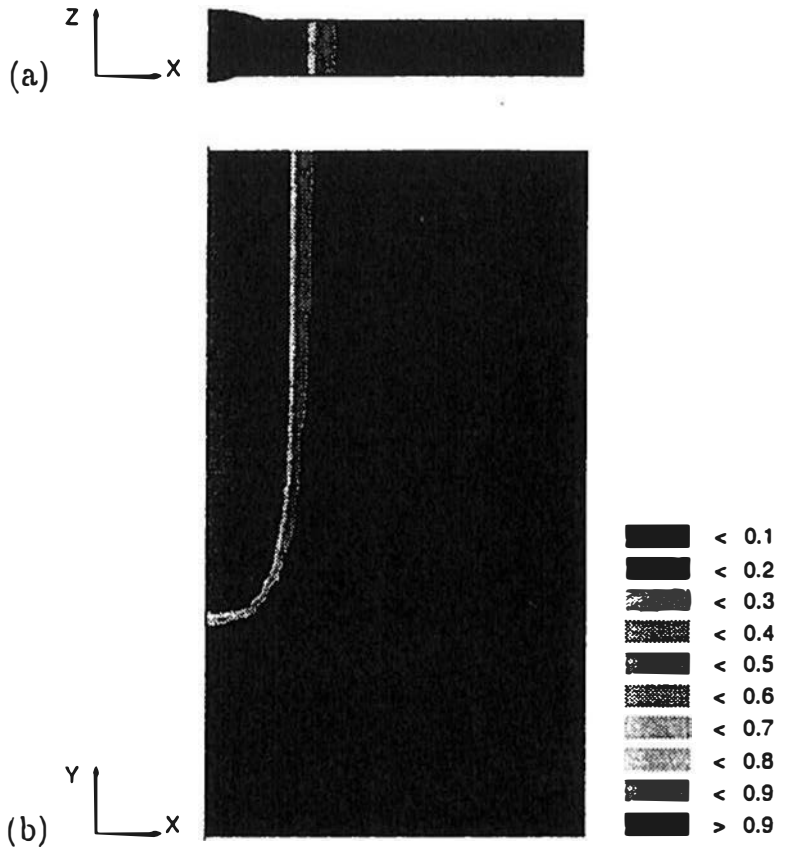

Figure 7. Contours of recrystallised fraction for the transverse model (a) and the longitudinal model (b).

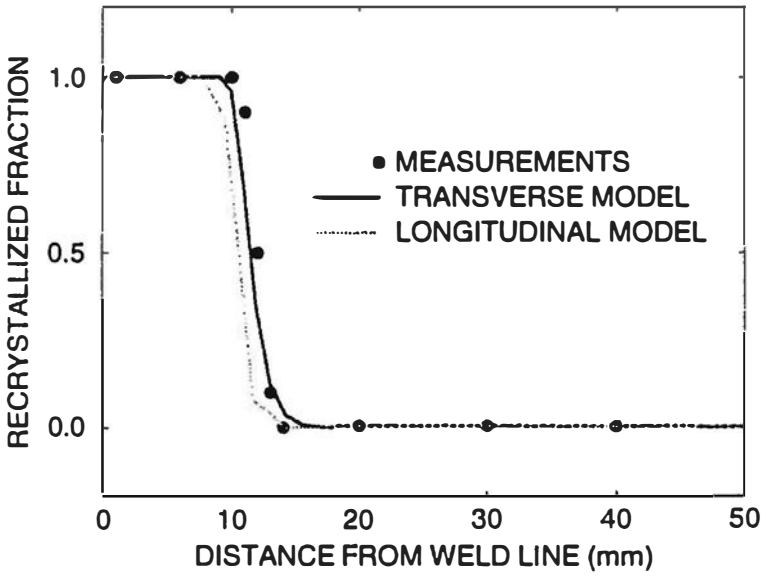

Figure 8. Microstructure distribution.

solution is obtained by a second order Runge–Kutta scheme. The initial metallurgical conditions are assumed without recrystallisation. Contours plotted on Fig. 7 and final structure on Fig. 8 show a good agreement between model predictions and measurements. The total HAZ width is about 24 mm.

MECHANICAL CALCULATION

Based on the temperature and structural distribution previously obtained, stresses are calculated using elastoplastic constitutive Equations (20) to (23). Stresses are analysed under generalised plane strain assumption for transverse model and under plane stress assumption for the longitudinal model. The calculated longitudinal σ_{yy} and transverse σ_{xx} residual stresses show a profile similar to that obtained by X-ray diffraction (Fig. 9) and the hole-drilling techniques (Fig. 10). Calculated stresses, however, are overestimated because of the two-dimensional modelling assumption. Indeed, generalised plane strain or plane stress assumptions lead inevitably to overestimation of stresses. Since the plates are thin and not clamped in the (OXY) plane, the transverse stress is very low. Concerning longitudinal stress, the centre of the weldments is under tension because its contraction is partly constrained by neighbouring parts which cool at a slower rate. To satisfy equilibrium, the longitudinal stress decreases and becomes negative far from the weld line. Recrystallisation occurring in the HAZ brings down the longitudinal stress because of decreasing of yield strength.

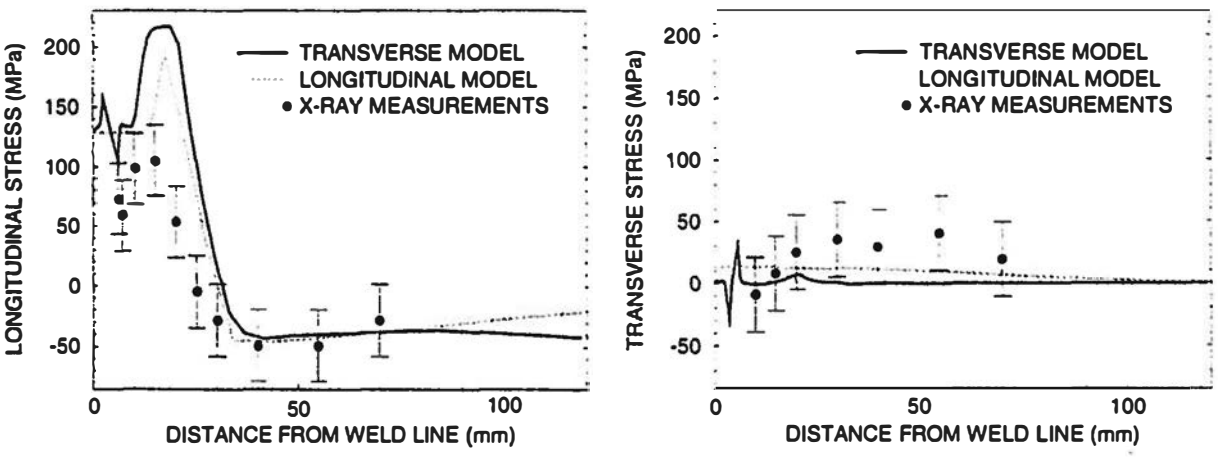

Figure 9. Calculated and X-ray measured stress distribution.

CONCLUSION

An arc welding model based on finite element techniques was used in conjunction with kinetic relationships developed to represent recrystallisation and its mechanical effects during welding. Based on accurate temperature-dependent thermal properties and metallurgical characterisations, temperature history and final microstructure have been quantitatively well predicted. Two simple and complementary 2D models gave qualitative stress distributions. The longitudinal stress is indeed overestimated by calculations because of the plane–strain or plane–stress hypothesis. However, comparisons between predictions and measurements are satisfactory. A quantitative determination would require a 3D simulation which remains computationally time-consuming.

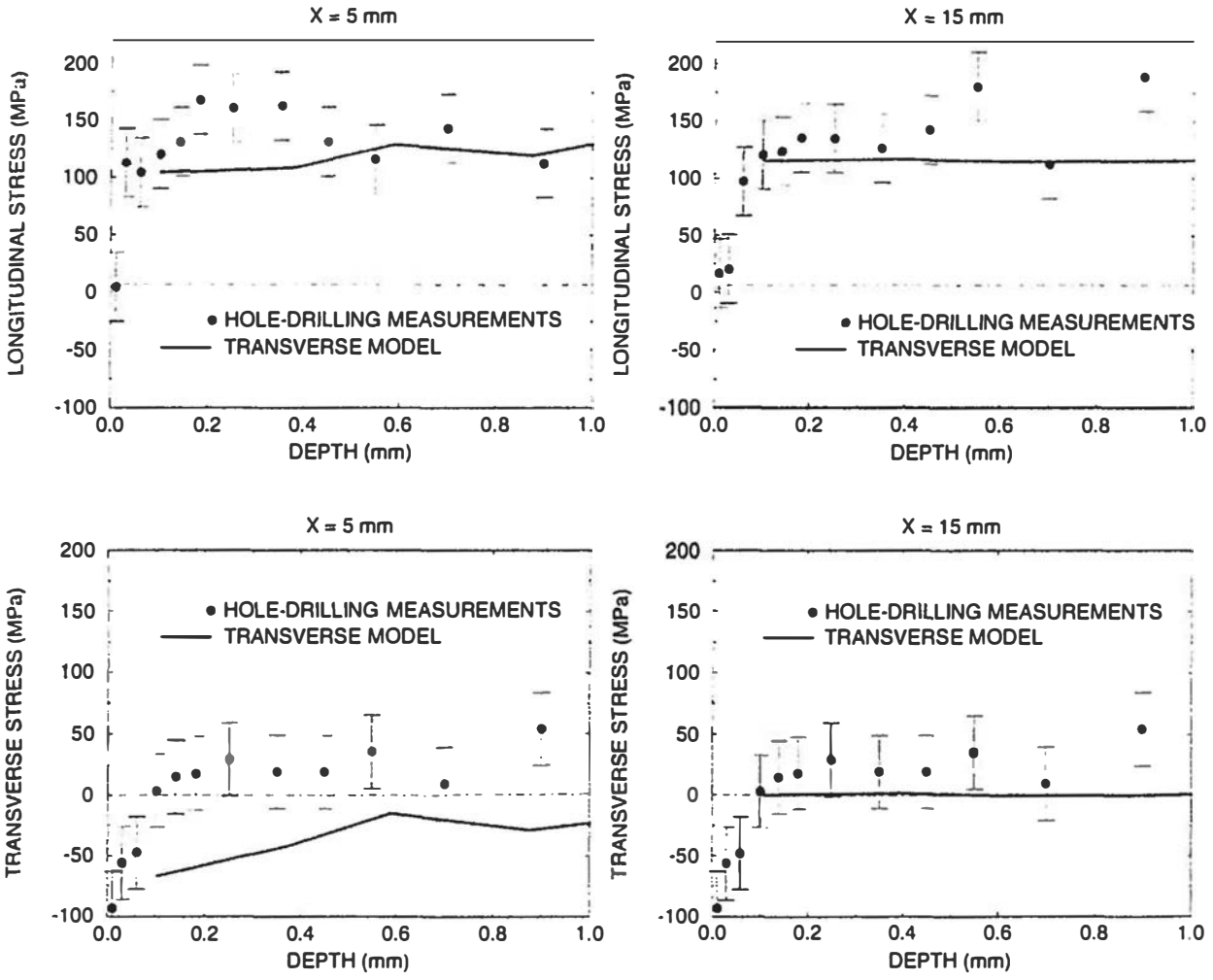

Figure 10. Calculated and hole-drilling measured stress distribution at 5 and 15 mm from weld line.

ACKNOWLEDGEMENTS

We are grateful to PECHINEY CRV (France) for financing this research. It also provided metallurgical characterisations. Mechanical tests have been carried out at ENSMP (Mines de Paris - France) and residual stresses measurements were made at ENSAM and CETIM (Paris - France).

REFERENCES

1. R.P. MARTUKANITZ: 'Modelling of the Heat-affected Zone of Aluminium Arc Welds', *ASM International*, Alcoa Laboratories, Pennsylvania, 1986, 193–201.
2. H.R. SHERCLIFF and M.F. ASHBY: 'A Process Model for Age Hardening of Aluminium Alloys, I The Model', *Acta Metall. Mater.*, 1990, **38**, (2), 1789–1802.
3. H.R. SHERCLIFF and M.F. ASHBY: 'A Process Model for Age Hardening of Aluminium Alloys, II Application of the Model', *Acta Metall. Mater.*, 1990, **38**,(10), 1803–1812.
4. O.R. MYHR and Ø. GRONG: 'Process Modelling Applied to 6082-T6 Aluminium Weldments, I Reaction Kinetics', *Acta Metall. Mater.*, 1991, (39), **11**, 2693–2702.
5. O.R. MYHR and Ø. GRONG: 'Process Modelling Applied to 6082-T6 Aluminium Weldments, II Applications of the Model', *Acta Metall. Mater.*, 1991, (39), **11**, 2703–2708.
6. T. INOUE and Z. WANG: 'Coupling Between Stress, Temperature and Metallic Structures During Processes Involving Phase Transformations', *Materials Science and Technology*, 1985, **1**, (10), 845–850.
7. C.R. BROOKS: 'Heat Treatment, Structure and Properties of Nonferrous Alloys, *American Society for Metals*, Ohio, 1982.
8. P.G. SHEWMON: *Transformation in Metals*, Mc-Graw Hill, 1969.
9. M. AVRAMI: Kinetics of Phase Change : I General Theory', *J. Chem. Phys.*, 1939, **7**, 1103–1113.
10. M. AVRAMI: 'Kinetics of Phase Change : II Transformation Time Relations for Random Distribution of Nuclei', *J. Chem. Phys.*, 1940, **8**, 212–224.
11. J.W. CAHN: 'Transformation Kinetics During Dontinuous Cooling', *Acta Metallurgica*, 1956, **4**, 572–575.
12. E. SARRAZIN: 'Modélisation du Soudage d'Alliages d'Aluminium, Ph.D. Thesis, Ecole Polytechnique, Palaiseau, 1995.